Electronic supplementary materials *Mendeleev Commun.*, 2025, **35**, 362–363

Effect of macrocycle stereoisomerism on extraction of Li^+ cations from chloride media by solutions of dicyclohexano-14-crown-4 in 1,1,7-trihydrododecafluoroheptanol

Olga A. Zakurdaeva, Andrey F. Asachenko, Maxim A. Topchiy and Sergey V. Nesterov

Content

1. Efficiency of Me^+ extraction

The efficiency of Li^+ and K^+ extraction from *single*- and *two*-component solutions was determined as an equilibrium concentrations of Me^+ cations in organic phase $[Me^+_{org}]^{eq}$. In the first case, the initial aqueous phase contained only one component – either LiCl or KCl. In the second case, *two*-component solution was used with LiCl concentration of 0.1 M and that of KCl in the range from 0.5 to 3 M (Figure S1, the error bars represent the confidence interval at P = 0.95 and n = 3).

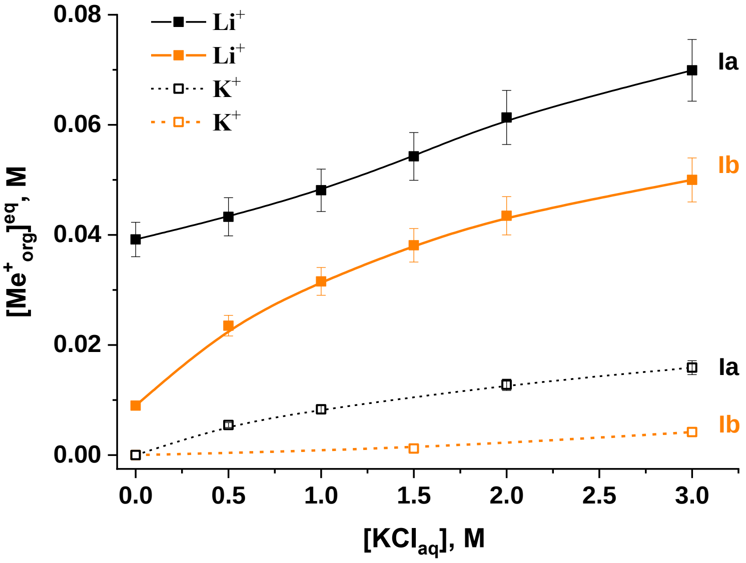

Figure S1 Efficiency of Li^+ and K^+ extraction from *two-component* aqueous phase containing LiCl ($[Li^+_{aq}]^{init}$ =0.1 M) and KCl ($[K^+_{aq}]^{init}$ = 0–3 M) with the solutions of **1a** (*cis-syn-cis*-DCH14C4) and **1b** (*cis-anti-cis*-DCH14C4) in 1,1,7-trihydrododecafluoroheptanol ($[DCH14C4_{org}]^{init}$ = 0.1 M). Volume a/o ratio was 1:1

1.1 Distribution ratio (D_{Me})

The distribution ratio of Me^+ (D_{Me}) were calculated using the equations:

$$D_{Me} = [Me^+_{org}]^{eq}/[Me^+_{aq}]^{eq},$$

$$[Me^+_{aq}]^{eq} = [Me^+_{aq}]^0 - [Me^+_{org}]^{eq},$$

where $[Me^+_{org}]^{eq}$ and $[Me^+_{aq}]^{eq}$ are equilibrium concentrations of Me^+ cations in organic and aqueous phases, respectively. $[Me^+_{aq}]^0$ is the initial concentration of Me^+ in aqueous phase.

The values of D_{Me} were averaged based on the results of three parallel tests.

1.2 Ligand loading capacity (CE%$_{Me}$)

$CE\%_{Me} = [Me^{+}_{org}]^{eq}/[CE_{org}]^{0} \cdot 100\%$,

where $[Me^{+}_{org}]^{eq}$ and $[CE_{org}]^{0}$ are equilibrium concentrations of Me^{+} and initial concentration of CE in organic phase.

The measured parameters of the extraction efficiency ($[Me^{+}_{org}]^{eq}$, $CE\%_{Me}$, D_{Me}) are given in Table S1.

Table S1 – Efficiency of Li^{+} and K^{+} extraction from *single*- and *two*-component aqueous solutions by 0.1 M solutions of individual stereoisomers of DCH14C4 in 1,1,7-trihydrododecafluoroheptanol

Initial aqueous phase	**Extraction efficiency parameter**	**Li^{+}**		**K^{+}**	
		cis-syn-cis- DCH14C4	*cis-anti-cis-* DCH14C4	*cis-syn-cis-* DCH14C4	*cis-anti-cis-* DCH14C4
Single-component aqueous solutions					
0.1 M LiCl	$[Me^{+}_{org}]^{eq}$	$(3.8\pm0.3)\cdot10^{-2}$ *	$(9.4\pm0.3)\cdot10^{-3}$		
	D_{Me}	0.64	0.1		
	$CE\%_{Me}$	38%	9%		
0.5 M LiCl	$[Me^{+}_{org}]^{eq}$	$(8.6\pm0.3)\cdot10^{-2}$	$(5.8\pm0.8)\cdot10^{-2}$		
	D_{Me}	0.2	0.1		
	$CE\%_{Me}$	87%	58%		
3 M LiCl	$[Me^{+}_{org}]^{eq}$	$(9.6\pm0.7)\cdot10^{-2}$	$(9.7\pm0.7)\cdot10^{-2}$		
	D_{Me}	$3.4\cdot10^{-2}$	$3.4\cdot10^{-2}$		
	$CE\%_{Me}$	96%	97%		
0.5 M KCl	$[Me^{+}_{org}]^{eq}$			$2.5\cdot10^{-2}$	$3.3\cdot10^{-4}$
	D_{Me}			$5.2\cdot10^{-2}$	$6.6\cdot10^{-4}$
	$CE\%_{Me}$			25%	0.3%
3 M KCl	$[Me^{+}_{org}]^{eq}$			$5.4\cdot10^{-2}$	$3.8\cdot10^{-3}$
	D_{Me}			$1.8\cdot10^{-2}$	$1.3\cdot10^{-3}$
	$CE\%_{Me}$			54%	4%
Two-component aqueous solution					
0.1 M LiCl + 3 M KCl	$[Me^{+}_{org}]^{eq}$	$7.0\cdot10^{-2}$	$5.1\cdot10^{-2}$	$1.6\cdot10^{-2}$	$4.0\cdot10^{-3}$
	D_{Me}	2.3	1.0	$5.3\cdot10^{-3}$	$1.4\cdot10^{-3}$
	$CE\%_{Me}$	70%	50%	15%	4%

*** -** the confidence interval at P = 0.95 and n = 3 is given in parentheses.

2. Selectivity of Li^+/K^+ removal

A selectivity coefficient ($\alpha_{Li/K} = D_{Li}/D_K$) was used as a parameter characterizing the selectivity of lithium extraction from *two-component* aqueous solutions (Figure **S2**, the error bars represent the confidence interval at P = 0.95 and n = 3).

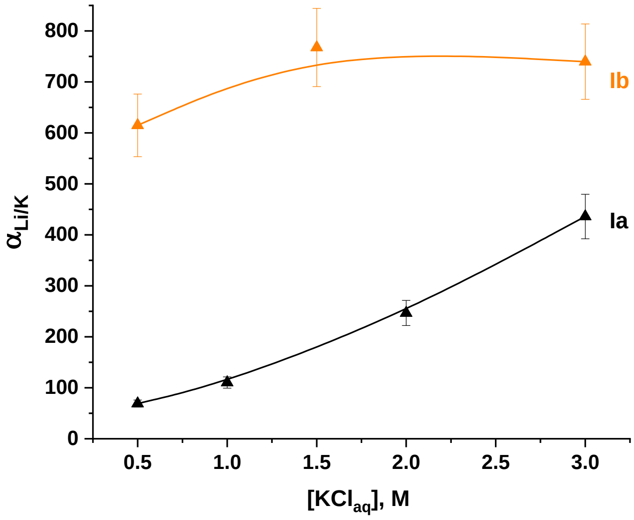

Figure S2 Selectivity of Li^+/K^+ removal from *two-component* aqueous solutions containing 0.1 M LiCl and 0.5-3 M KCl with 0.1 M solutions of **1a** and **1b** in 1,1,7-trihydrododecafluoroheptanol

3. Equilibrium concentration of metal cation in organic phase ($[Me^+_{org}]^{eq}$)

The procedure of $[Me^+_{org}]^{eq}$ determination included several stages: extraction of Me^+ from *single*- or *two*-component solutions with 0.1 M DCH14C4 solution in 1,1,7-trihydrododecafluoroheptanol; re-extraction of Me^+ with deionized water and measuring the Me^+ concentration in the re-extract using ion-selective electrodes. At the extraction stage, the volume ratio of the aqueous and organic phases was 1:1, mixing was carried out using a laboratory shaker PE-6410 (Ekros, Russia) for 60 minutes. After mixing, the phases were separated on a laboratory centrifuge PE-6926 (Ekros, Russia) at 2500 rpm, the phase separation time was 5 minutes. In the case of extraction from single-component aqueous solutions, an aliquot of the organic phase (V_{aliq}^{org}) was taken and the extracted Me^+ was re-extracted with deionized water (20 ml) with a resistivity of ~18 MOhm·cm. In case of two-component solutions (LiCl + KCl), two aliquots of the organic phase were separated followed by re-extraction of the Me^+ cations from each of aliquot with 20 ml of deionized water. Accordingly, these resulting re-extracts including Li^+ and K^+ (two-component re-extracts), were analyzed separately on the Li^+ and K^+ content. The volume of aliquots of the organic phase at the re-extraction stage (V_{aliq}^{org}) was varied from 1 to 18 ml, depending on the type of cation to be determined (Li^+ or K^+) and the composition of the initial aqueous phase, so that the Me^+ concentration in the re-extract was within a working range for the corresponding ion-selective electrode. The V_{aliq}^{org} required for this purpose was determined for each system from the preliminary tests at minimum and maximum concentrations of the salts in the initial aqueous phase.

The concentrations of Li^+ and K^+ ions in the obtained re-extracts were measured using lithium- and potassium-selective electrodes "Alice-142Li" and "Alice-121K" (Measuring Equipment Ltd., Russia) and ionometer "Expert-001-3" (Econix-Expert, Russia). The 0.05% aqueous solution of NH_3 (45 μl) was added to all analyzed samples to obtain and maintain pH value of ~8. The pH of the resulting mixtures was controlled using a glass combined electrode ESC-100603/7. Ion-selective electrodes were pre-calibrated using *one*- and *two*-component solutions (LiCl or LiCl + KCl) with a known concentration in the range from $1 \cdot 10^{-5}$ to 0.1 M. Calibration curves are given in Figure S3. The calibration equations $E_{Me+} = a + b \cdot pX$, where $pX = -\log[Me^+]$, were obtained by linear approximation of experimental points in the linear portion of the emf=*f*[Me^+] function. The compositions of the calibration solutions, the linearity ranges and the coefficients of the calibration equation are given in Table S2. To determine the concentration of Me^+, the emf of the corresponding re-extract was measured and [$Me^+_{re\text{-}extr}$] was calculated using the calibration equation. The equilibrium concentration in the organic phase [Me^+_{org}] was calculated taking into account the volumes of the aliquot of the organic phase and water taken for the re-extraction of Me^+ using the following equation:

$$[Me^+_{org}]^{eq} = [Me^+_{re\text{-}extr}] \cdot (20/V_{aliq}^{org})$$

Table S2 – Linear approximation coefficients for the calibration dependencies of the ion-selective electrodes

Electrode	**Calibration solutions**	**Linearity range of E_{Me+} ***	**Linear approximation coefficients E_{Me+} = a + b·pX**	
			a	**b**
Li-selective	Single-component LiCl ($1 \cdot 10^{-4}$ – 0.1 M)	$1 \cdot 10^{-3}$ – 0.1 M	-(2496±3)	-(56±1)
	Two-component LiCl ($1 \cdot 10^{-4}$ – 0.1 M) and KCl ($2.5 \cdot 10^{-3}$ M)	$3 \cdot 10^{-3}$ – 0.1 M	-(2493.7±0.4)	-(56.8±0.2)
К- selective	Single-component KCl ($1 \cdot 10^{-4}$ – 0.1 M)	$1 \cdot 10^{-4}$ – 0.1 M	499.5±2.2	-(55±1)
	Two-component KCl ($1 \cdot 10^{-5}$ – 0.1 M) and LiCl ($5 \cdot 10^{-2}$ M)	$1 \cdot 10^{-4}$ – 0.1 M	479±2	-(55±1)

* **-** operating range of the ion-selective electrode.

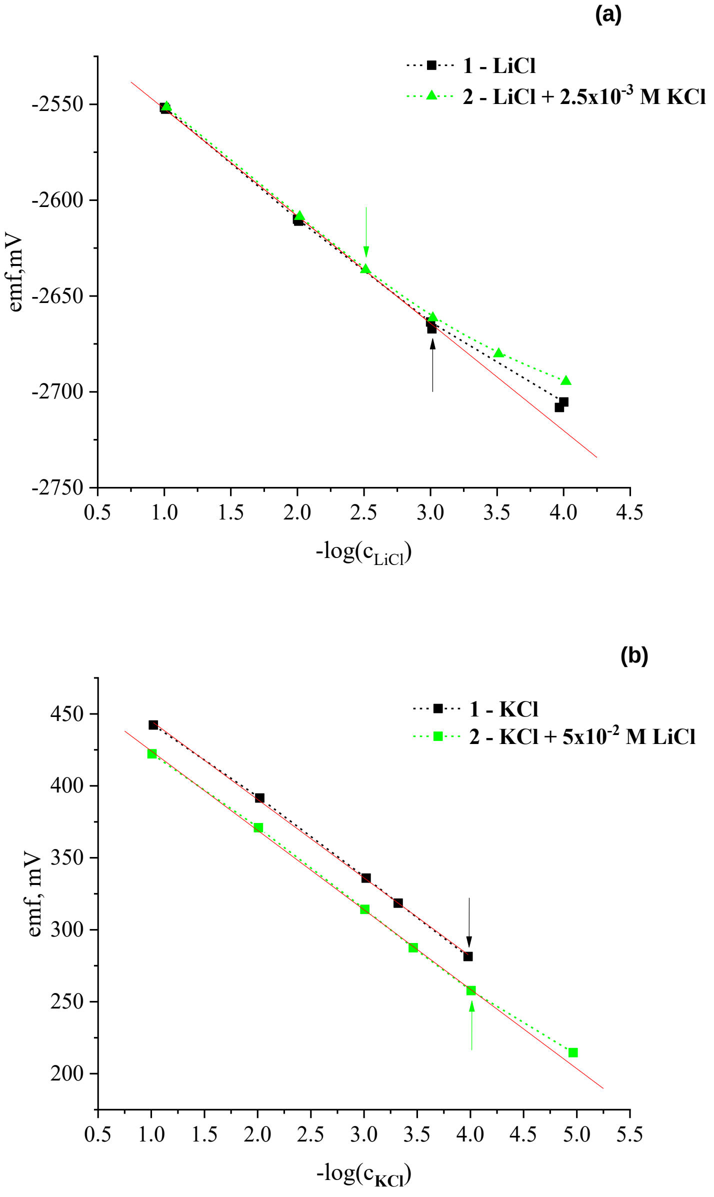

Figure S3 Calibration curves for (*a*) lithium-selective and (*b*) potassium-selective electrodes for single-component and two-component solutions. Red lines resulted from linear approximation of the experimental data. Black and green arrows point to lower limits of the linearity of EMF function

4. DCH14C4 distribution between organic solution and aqueous phase (ligand transfer to aqueous phase)

As a criterion of the extractant stability, the transfer of the macrocyclic ligand from the organic solvent to aqueous phase was chosen. It was quantified by the coefficient of CE distribution (K_d):

$$K_d(\mathrm{CE}) = [\mathrm{CE}]_{\mathrm{org}}/[\mathrm{CE}]_{\mathrm{aq}},$$

where $[\mathrm{CE}]_{\mathrm{org}}$ and $[\mathrm{CE}]_{\mathrm{aq}}$ represent the equilibrium concentrations of the macrocycle in the organic and aqueous phases, respectively. The equilibrium concentrations of CE in the aqueous phase were determined using a modification of extraction-spectrophotometric techniques published previously.**[S2,S3]** These techniques are based on the ability of CE to form the stable macrocyclic complexes with $\mathrm{Me}^{n+}\mathrm{A}^{-}_{n}$ salt in aqueous media, which can be quantitatively extracted into an organic solvent, with A^{-} being a colored anion.

0.1 M solutions of *cis-syn-cis*-DCH14C4 **1a** in 1,1,7-trihydrododecafluoroheptanol and 5.5 M aqueous solution of LiCl were used to determine the coefficient of CE distribution. At initial stage the organic and aqueous phases (o/a ratio was 1:10) were contacted for 60 min. After phase separation, the aqueous layer “saturated” with the crown ether was isolated and centrifuged for 5 min at 3500 rpm to remove the traces of the solvent. To determine the concentration of DCH14C4 in the resulting sample ($[\mathrm{CE}]_{\mathrm{aq}}$), the aliquot of this phase (V_{aliq} = 16.4 ml), 28.6 ml H_2O, 1 ml of $1.5\cdot10^{-3}$ M aqueous solution of lithium salt of bromothymol blue (Li·BTB) and 2.5 ml of toluene were mixed in a separation funnel for 15 min to complete the formation of the colored macrocyclic complex in the organic phase. The two-phase system was separated, the organic layer was isolated and additionally centrifuged for 5 min at 3500 rpm to remove the traces of the aqueous phase. The resulted toluene phase was analyzed by UV-Vis spectrometry, and the optical density of the solution of colored $\mathrm{Li}^{+}\cdot\mathrm{DCH14C4}\cdot\mathrm{BTB}^{-}$ complex was measured at 399.5 nm. The concentration of the macrocyclic complex in the toluene solution $[\mathrm{CE}]_{\mathrm{toluene}}$ and subsequently that of DCH14C4 in water $[\mathrm{CE}]_{\mathrm{aq}}$ were calculated using a calibration curve and equation $[\mathrm{CE}]_{\mathrm{aq}} = [\mathrm{CE}]_{\mathrm{toluene}} / (V_{\mathrm{aliq}}/V_{\mathrm{toluene}})$, respectively. The calibration curve was preliminary obtained by the same procedure except that 5.5 M LiCl solution was used instead of analyzed aqueous phase (V_{aliq}) and solutions of DCH14C4 in toluene with CE concentration in the range from $2.5\cdot10^{-5}$ to $1.5\cdot10^{-4}$ M – instead of toluene. The five “blank” tests (CE-free toluene) were carried out by the same way. The CE distribution tests were done in triplicate, and average value of $K_d(\mathrm{CE})$ of $(2.0\pm0.4)\cdot10^{5}$ was calculated.

5. Synthesis of DCH14C4, isolation of cis-syn-cis- and cis-anti-cis-isomers and their characterization

A 100 ml stainless-steel autoclave was charged with a magnetic stir bar, 50 ml of *n*-butanol, 12.5 g of dibenzo-14-crown-4 and 1.25 g of 5% Ru@Al_2O_3. The autoclave was flushed with nitrogen for 3 times and pressurized with hydrogen (70 atm). The reaction mixture was hydrogenated at 100 °C for 24 h. The autoclave was allowed to cool and vented; the reaction mixture (*n*-butanol, residual precursor, crude DCH14C4) was filtered to remove the catalyst. The filtrate was evaporated to dryness and the oily residue was purified by chromatography on silica gel (eluent was hexane–ethyl acetate). The solvent was removed from the fractions containing the corresponding products **1a,b**.

The individual stereoisomers of DCH14C4 **1a,b** were characterized by ^1H NMR, ^{13}C NMR, ^1H-^{13}C HSQC (hsqcedetgpsisp2.3), ^1H-^1H COSY (cosygpmfphpp), ^1H-^1H NOESY (noesygpphpp, mixing time 900 ms) NMR and High-Resolution Mass Spectrometry (HRMS). NMR spectra were obtained on a Bruker “Ascend 400” (400 MHz ^1H, 101 MHz ^{13}C). Coupling constants *J* are given in Hertz as positive values regardless of their real individual signs. The multiplicity of the signals is indicated as ‘‘s”, ‘‘d”, “t” or ‘‘m” for singlet, doublet, triplet or multiplet, respectively. High Resolution Mass Spectrometry spectra were measured using AB Sciex TripleTOF 5600+ equipped with a TurboV and PhotoSpray ion sources.

Thermal analysis (TGA/DSC) of the samples was performed using a simultaneous thermal analyzer NETZSCH STA 499 F3 Jupiter. The samples of DCH14C4 were heated in the temperature range from 30 to 500°C in Al_2O_3 crucibles with a lid provided with a hole in the center. The rate of heating was 10 °C/min. The analyzed samples were purged with argon at a flow rate of 30 ml/min. An empty crucible was used as a reference sample. The mass of the samples was 5-10 mg.

The FTIR spectra were measured using Nicolet iS50 FT-IR spectrometer with a Fourier transform with a resolution of 2 cm^{-1}. Samples in the form of a suspension in mineral oil placed between KBr plates were used for analysis. The spectra were recorded at room temperature. The FTIR spectrum of the mineral oil was previously measured and used as a background. The spectrum of the sample and the spectrum of the mineral oil were normalized to the intensity of the absorption band at 722 cm^{-1} being the characteristic band of exclusively mineral oil, and the background spectrum was subtracted.

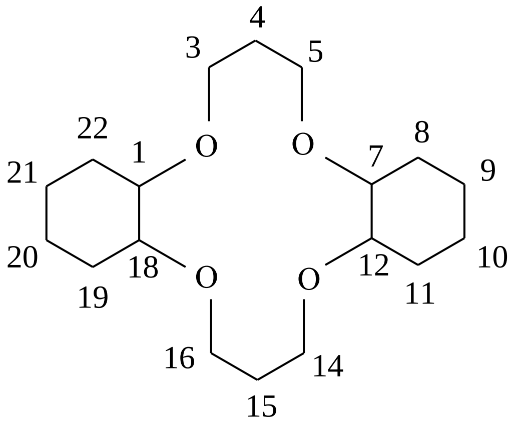

Table S3 Some characteristic parameters of the investigated DCH14C4 stereoisomers

DCH14C4	^{13}**C NMR** (101 MHz, Chloroform-*d*) δ					FTIR (C–O–C), cm^{-1}	Melting point
	C_1, C_7, C_{12}, C_{18}	C_3, C_5, C_{14}, C_{16}	C_4, C_{15}	C_8, C_{11}, C_{19}, C_{22}	C_9, C_{10}, C_{20}, C_{21}		
cis-syn-cis **1a**	78.16	64.35	30.97	28.03	24.23	1147, 1121, 1106	104°C
cis-anti-cis **1b**	76.13	63.83	30.94	27.84	22.33	1130, 1113, 1105	154°C

The interpretation of the ^{13}C NMR signals was carried out in accordance with the data of paper,[S1] the numbering of carbon atoms in the macrocycle is shown in the structural formula above.

5.1 HRMS and NMR spectra of cis-syn-cis-DCH14C4 **1a**

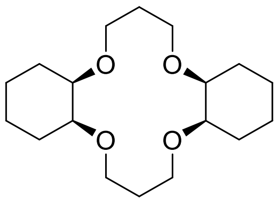

cis-syn-cis-DCH14C4 **1a**

^{1}H NMR (400 MHz, Chloroform-*d*) δ 3.77 – 3.57 (m, 8H), 3.57 – 3.44 (m, 4H), 1.87 – 1.68 (m, 8H), 1.68 – 1.48 (m, 8H), 1.34 – 1.17 (m, 4H).

^{13}C NMR (101 MHz, Chloroform-*d*) δ 78.18 , 64.35 , 30.97 , 28.03 , 22.43.

HRMS (m/z): calc. for $C_{18}H_{33}O_4^+$ $[M+H]^+$: 313.2379; found: 313.2378.

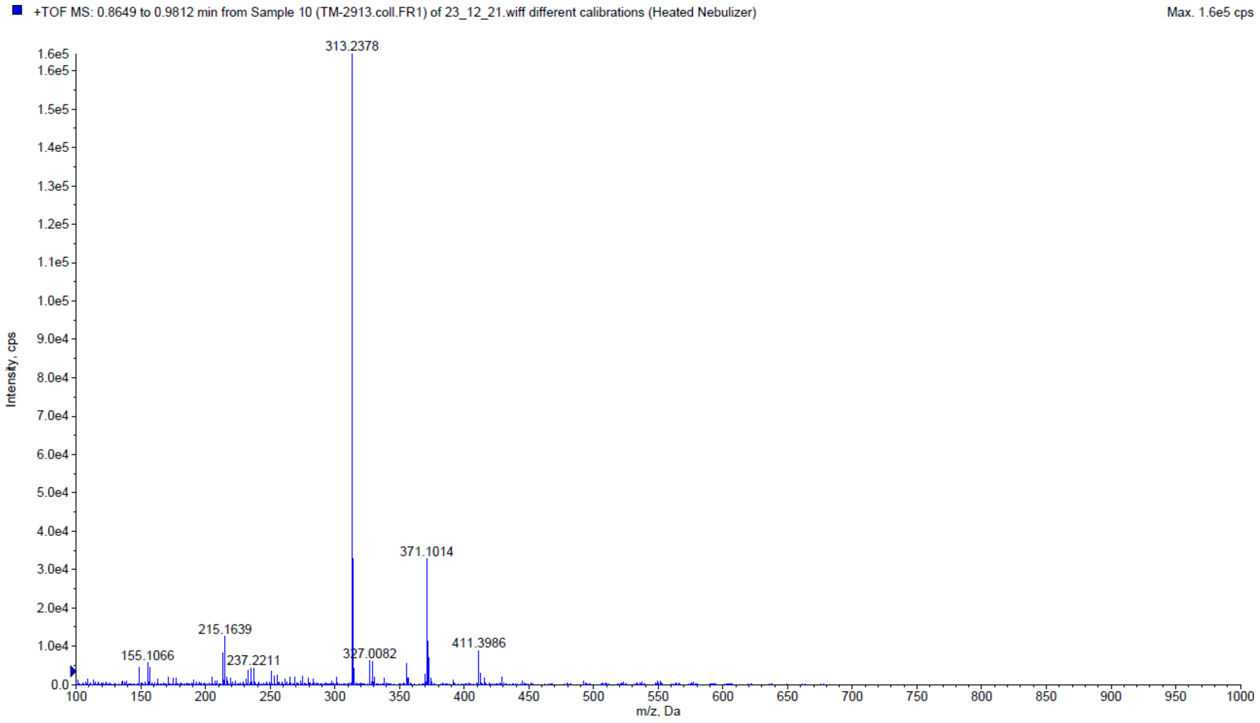

Figure S4 HRMS spectrum of *cis*-*syn*-*cis*-DCH14C4 **1a**

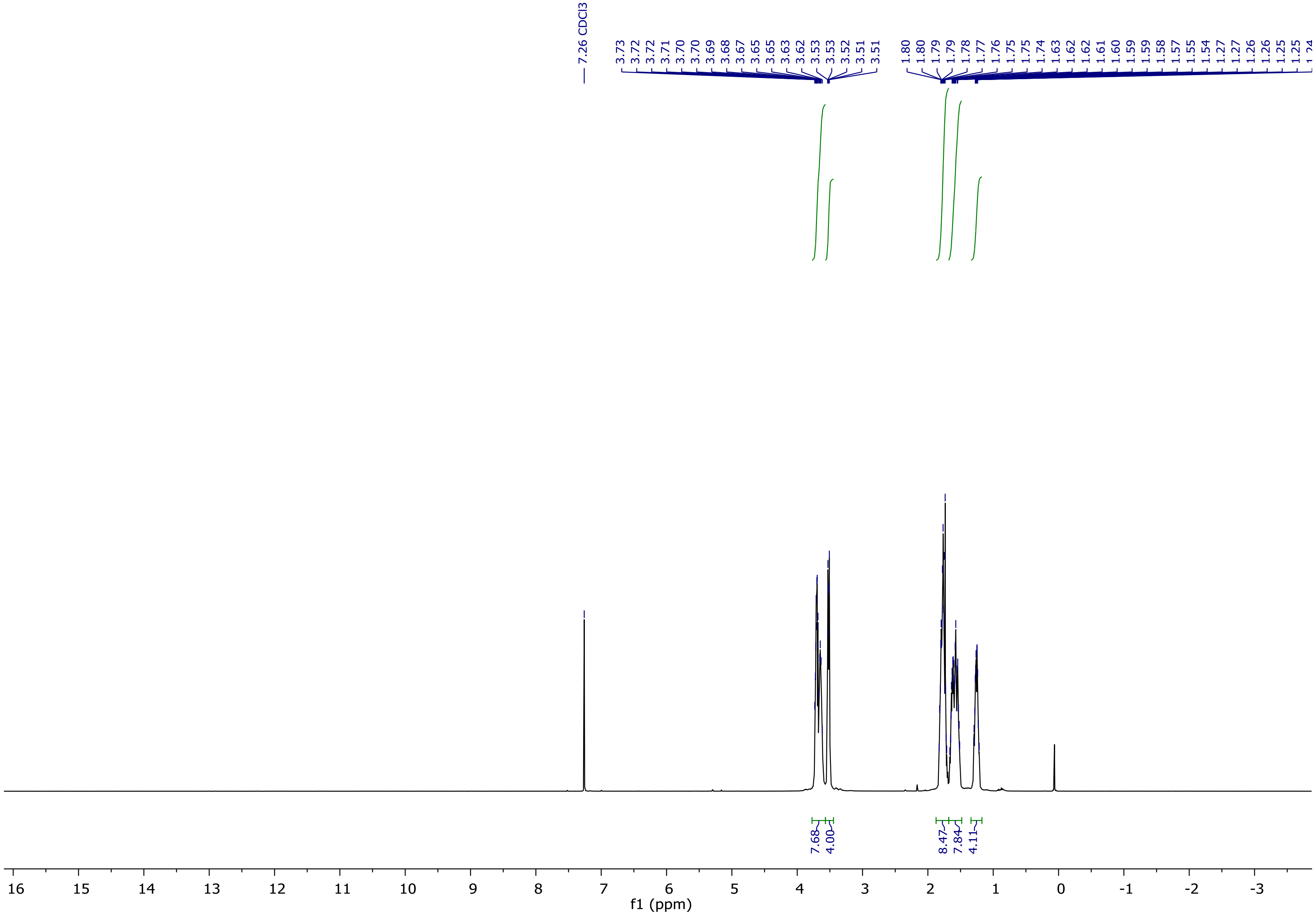

Figure S5 ^{1}H NMR of *cis*-*syn*-*cis*-DCH14C4 **1a**

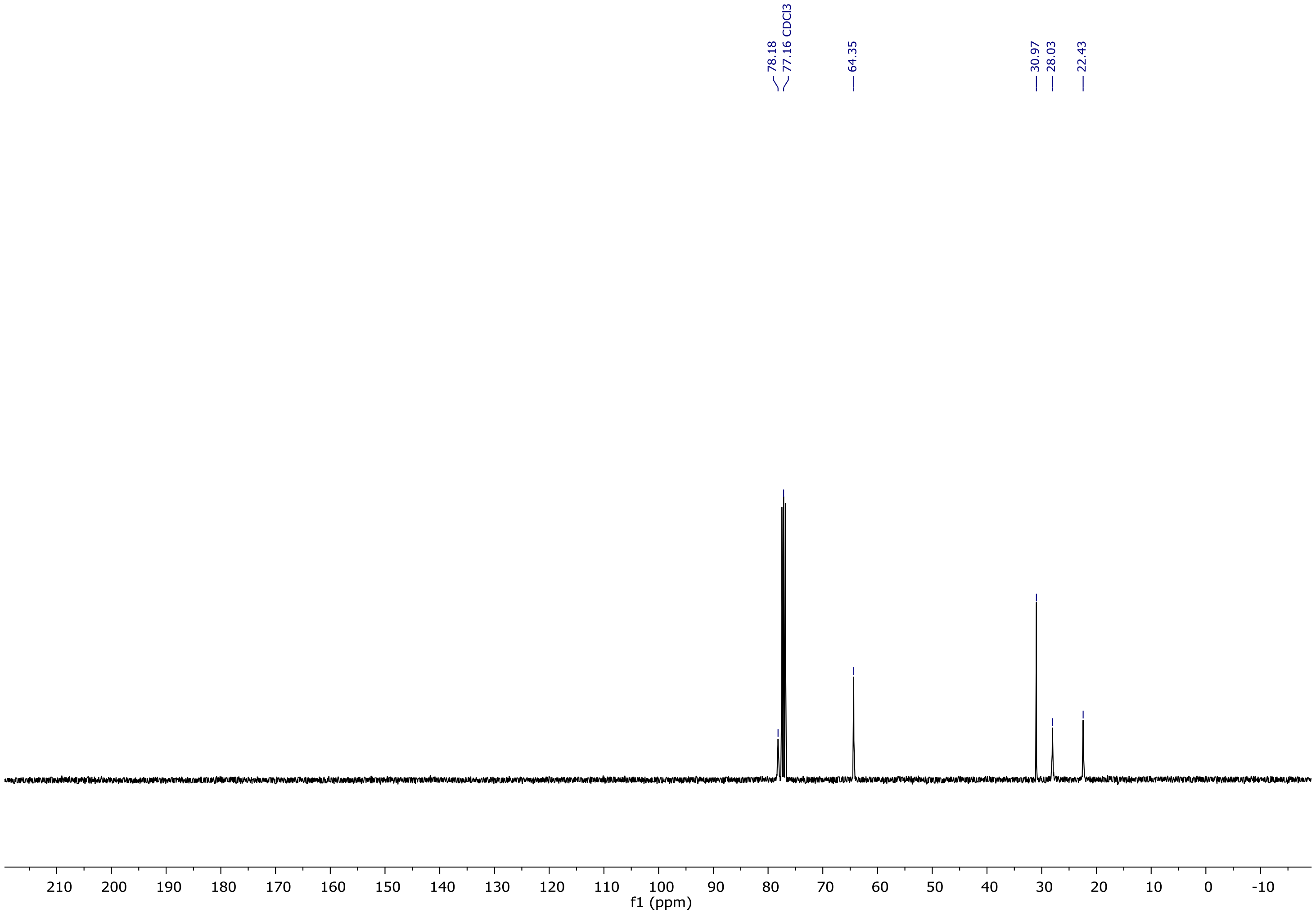

Figure S6 ^{13}C NMR of *cis*-*syn*-*cis*-DCH14C4 **1a**

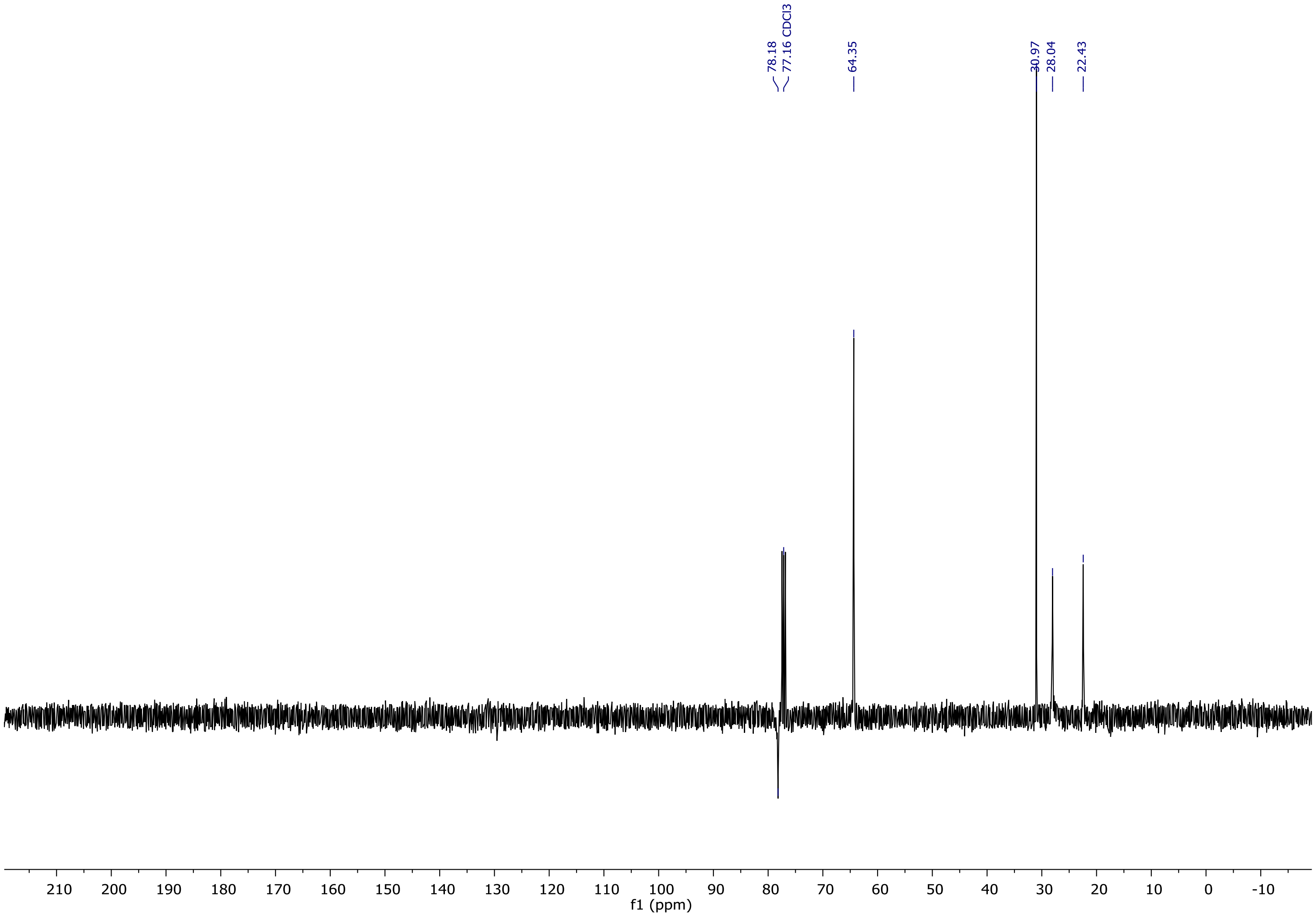

Figure S7 ^{13}C DEPTQ-135 NMR of *cis-syn-cis*-DCH14C4 b1a

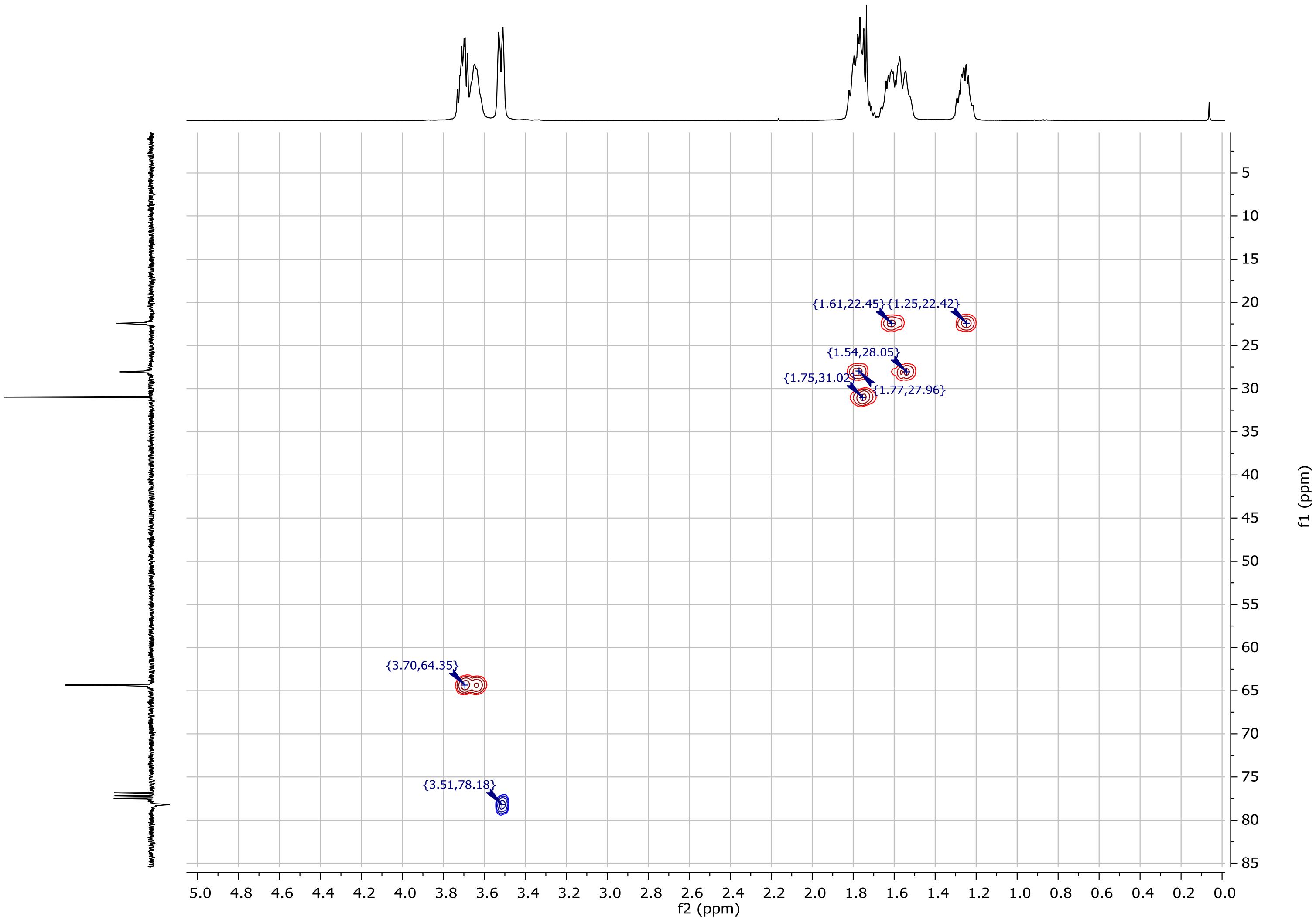

Figure S8 ^{1}H-^{13}C HSQC NMR of *cis*-*syn*-*cis*-DCH14C4 b1a

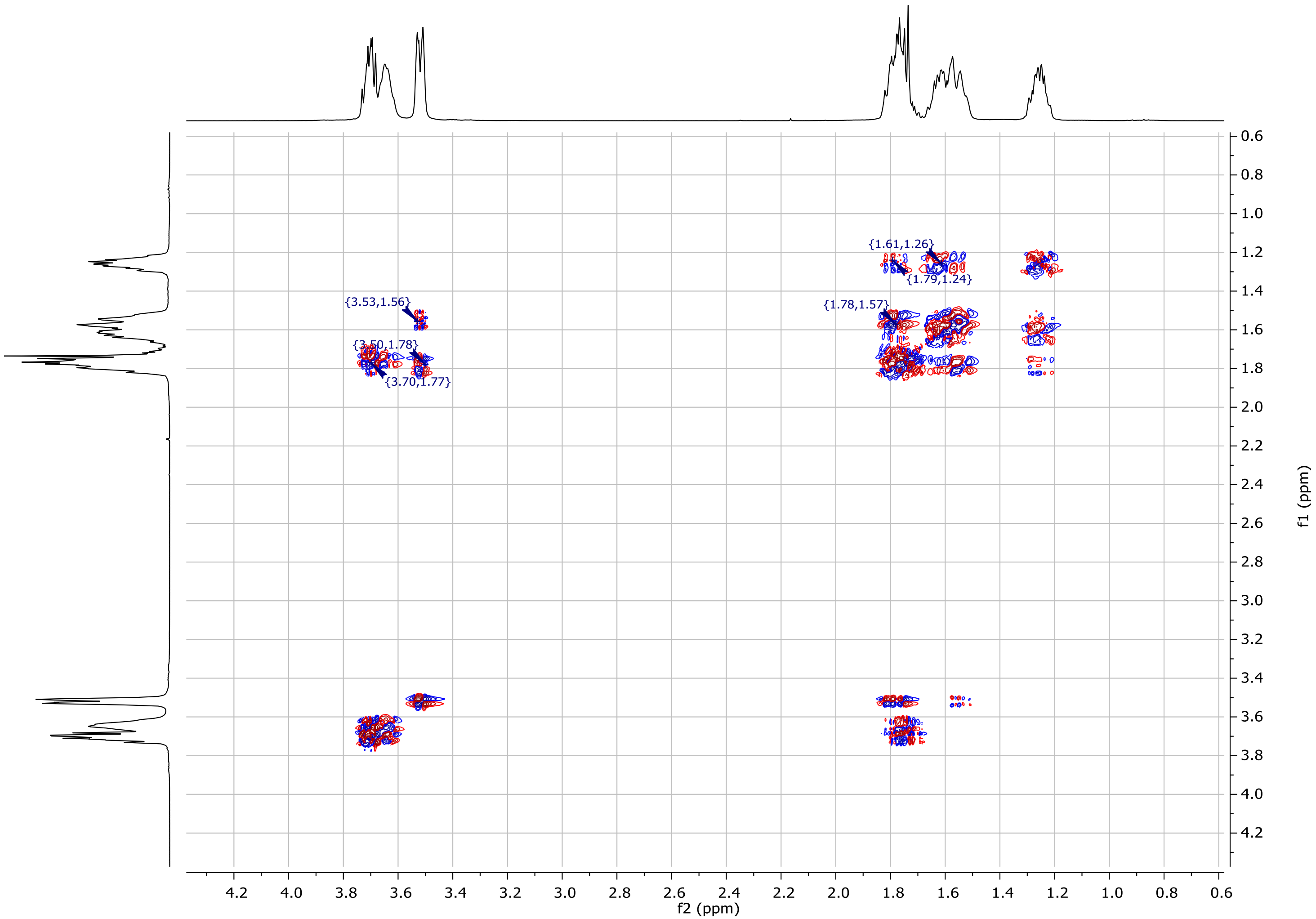

Figure S9 ^{1}H-^{1}H COSY NMR of *cis*-*syn*-*cis*-DCH14C4 **1a**

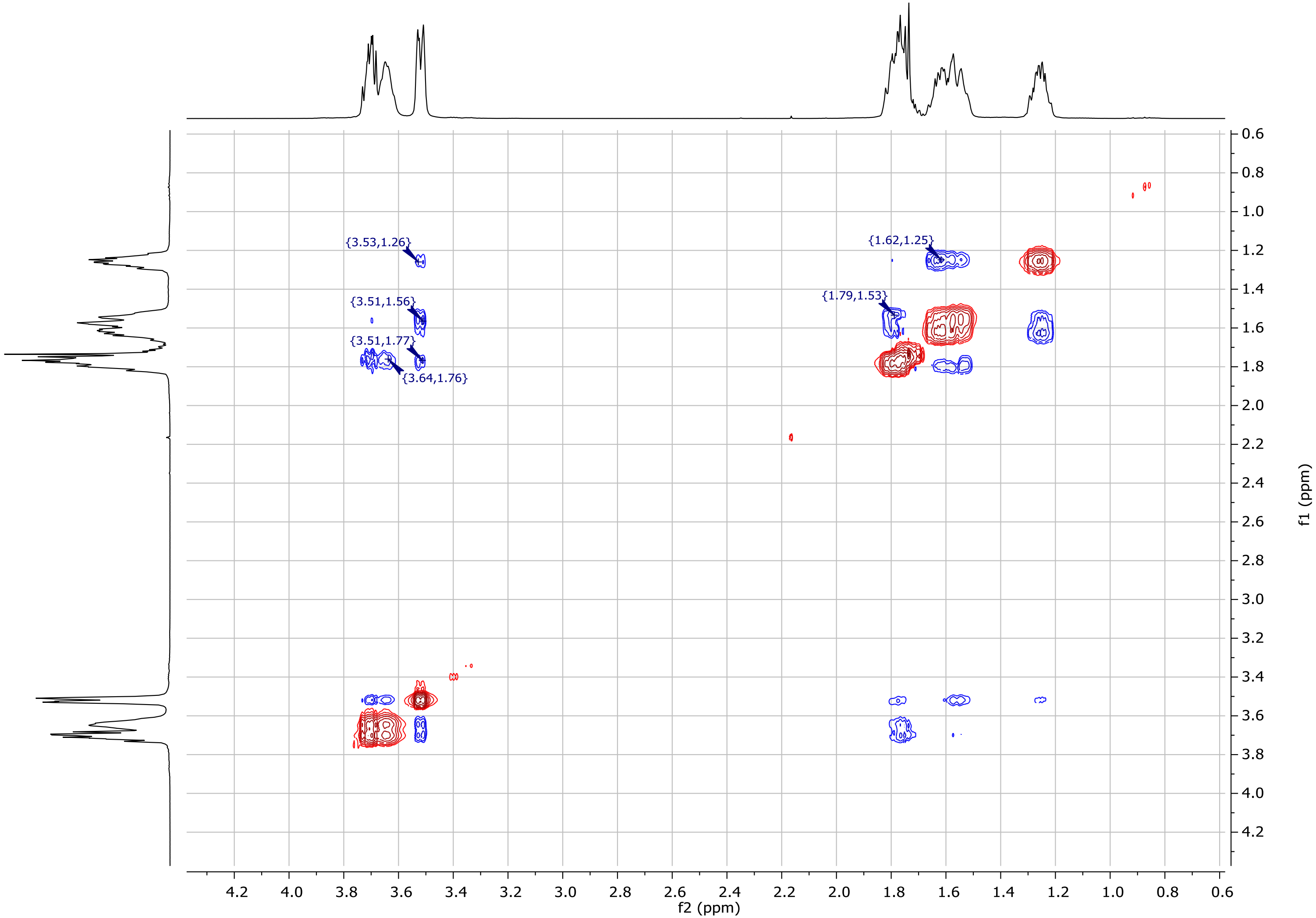

Figure S10 ^{1}H-^{1}H NOESY NMR of *cis-syn-cis*-DCH14C4 **1a**

5.2 HRMS and NMR spectra of cis-anti-cis-DCH14C4 **1b**

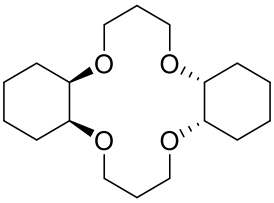

cis-anti-cis-DCH14C4 **1b**

^{1}H NMR (400 MHz, Chloroform-*d*) δ 3.81 – 3.68 (m, 4H), 3.56 – 3.46 (m, 4H), 3.45 – 3.30 (m, 4H), 1.92 – 1.76 (m, 8H), 1.63 – 1.53 (m, 4H), 1.41 – 1.23 (m, 8H).

^{13}C NMR (101 MHz, Chloroform-*d*) δ 76.13 (br. s) , 63.83 , 30.94 , 27.84 , 22.33.

HRMS (m/z): calc. for $C_{18}H_{33}O_4^+$ $[M+H]^+$: 313.2379; found: 313.2378.

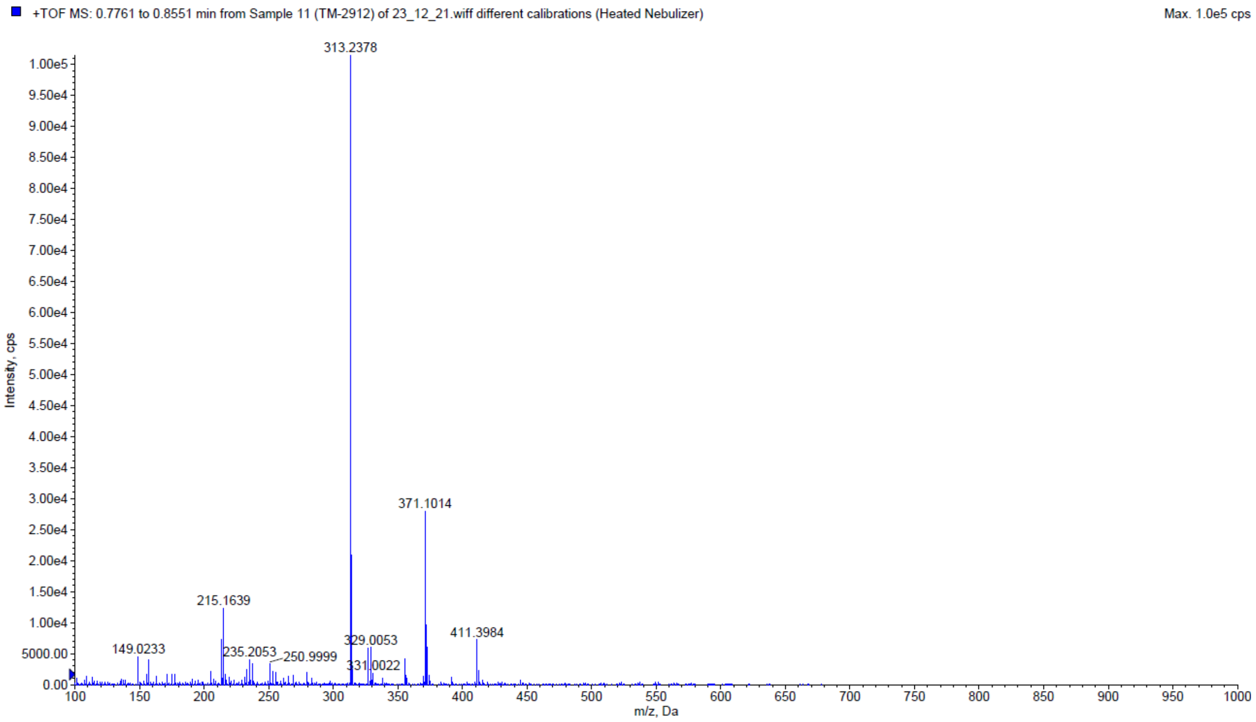

Figure S11 HRMS spectrum of *cis*-*anti*-*cis*-DCH14C4 **1b**

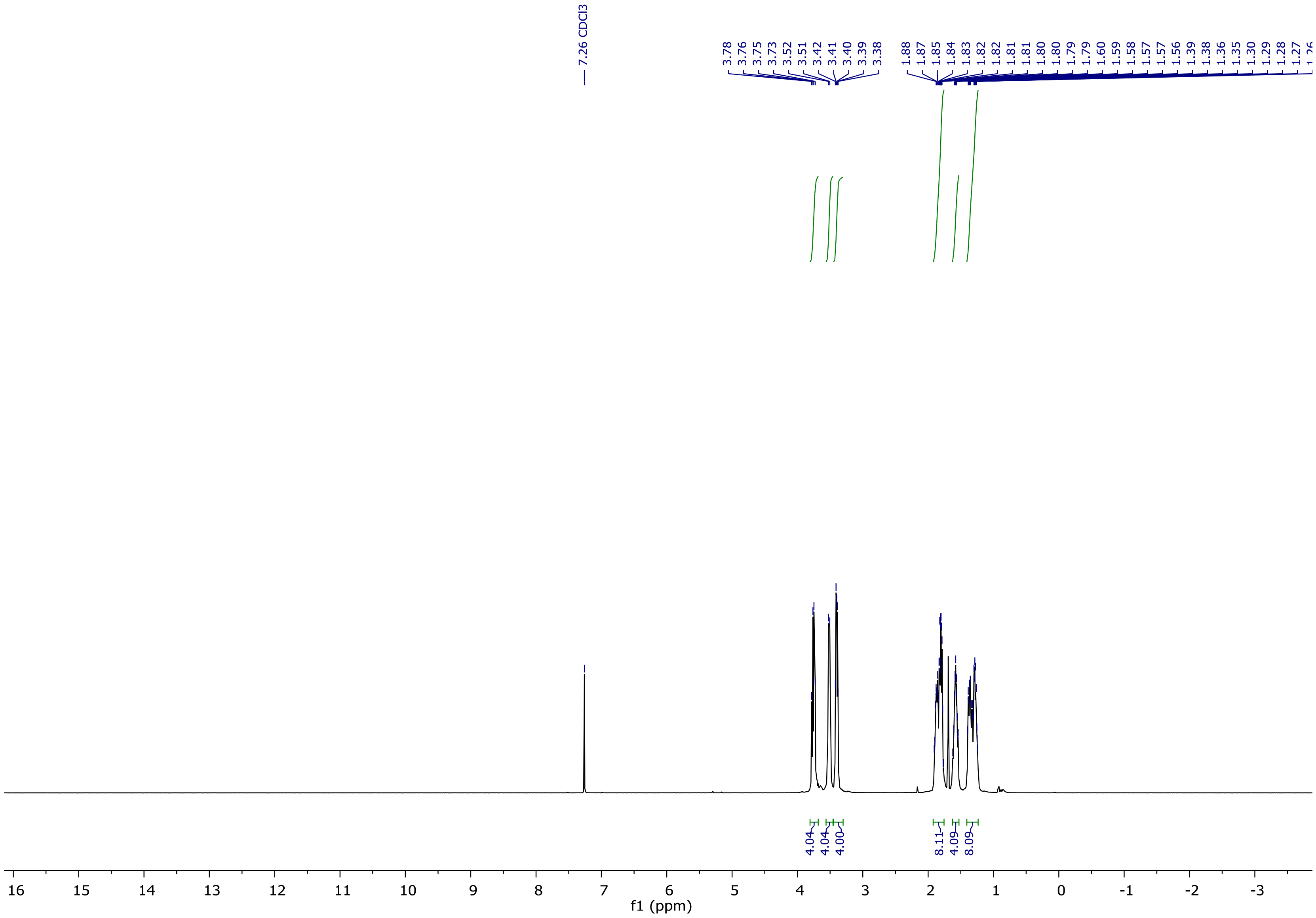

Figure S12 ^{1}H NMR of *cis*-*anti*-*cis*-DCH14C4 **1b**

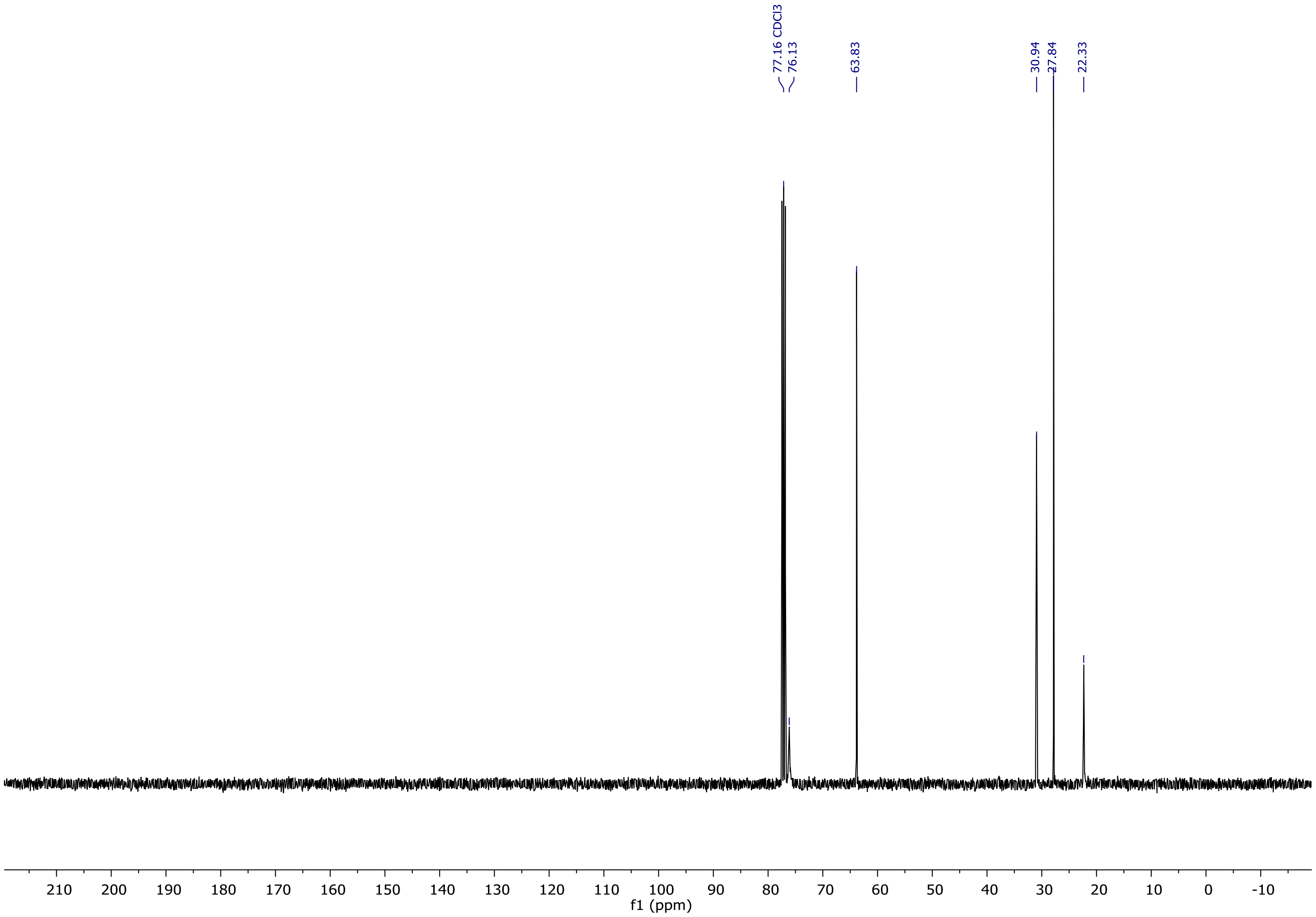

Figure S13 ^{13}C NMR of *cis*-*anti*-*cis*-DCH14C4 **1b**

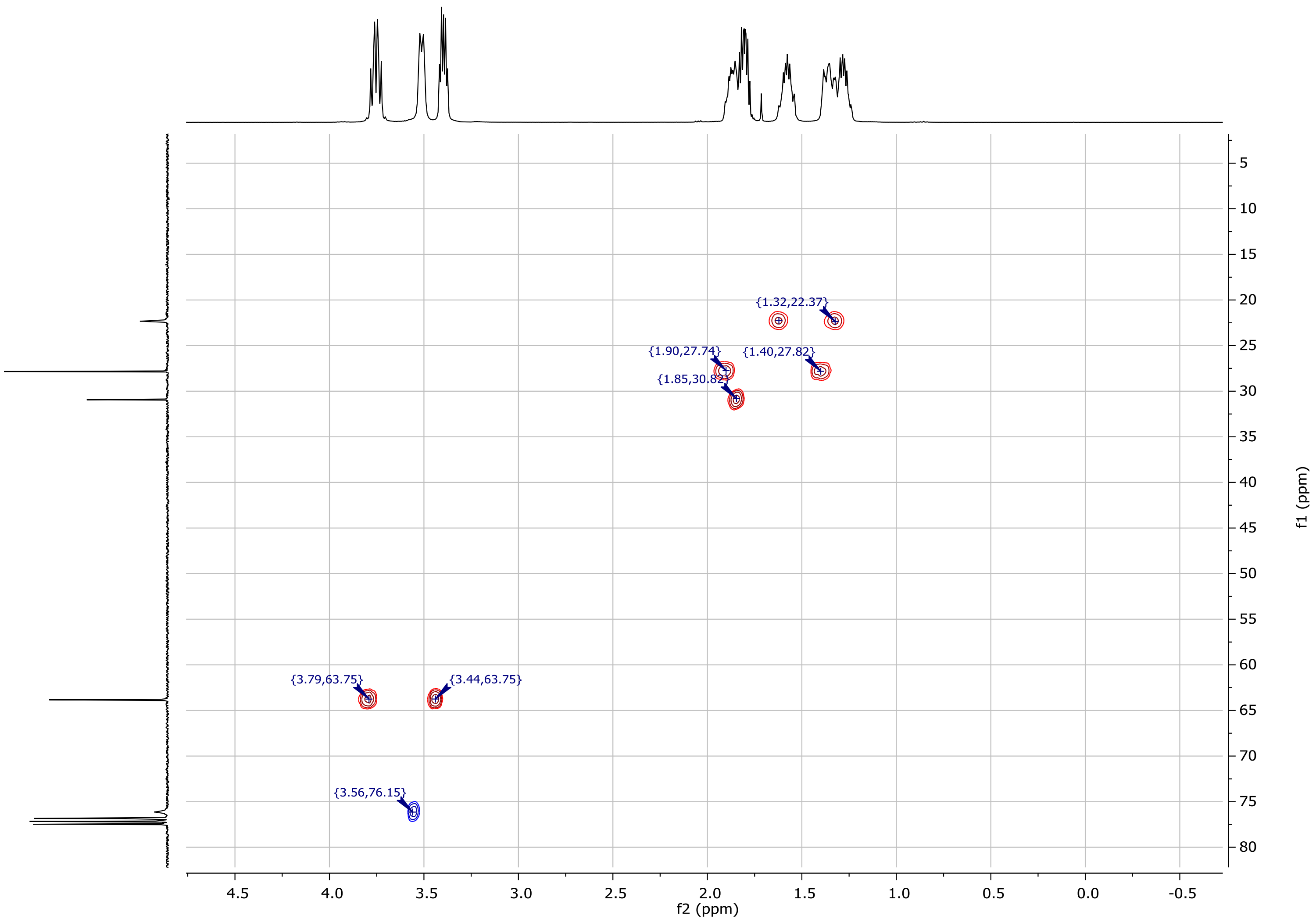

Figure S14 ^{1}H-^{13}C HSQC NMR of *cis-anti-cis*-DCH14C4 **1b**

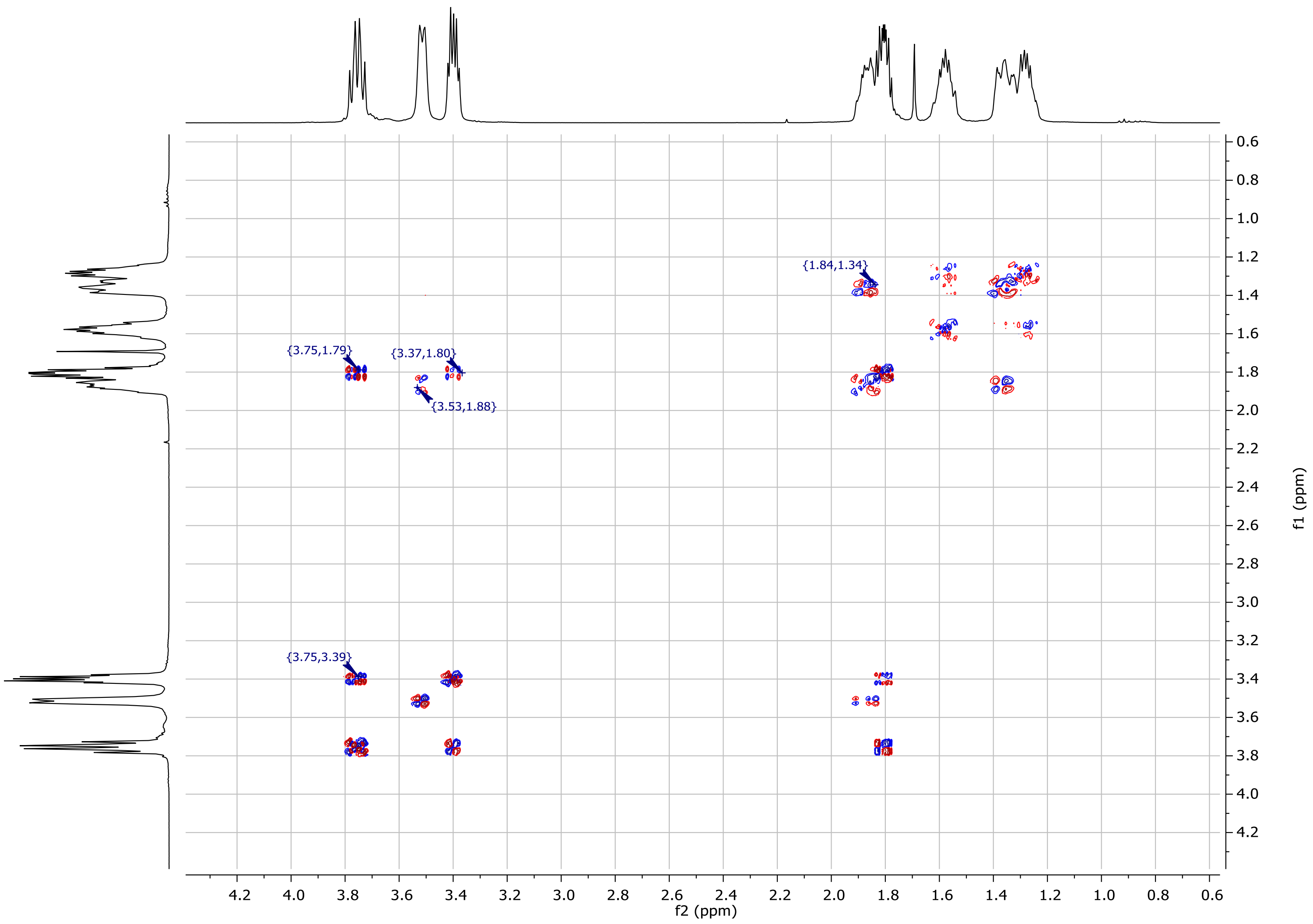

Figure S15 ^{1}H-^{1}H COSY NMR of *cis*-*anti*-*cis*-DCH14C4 **1b**

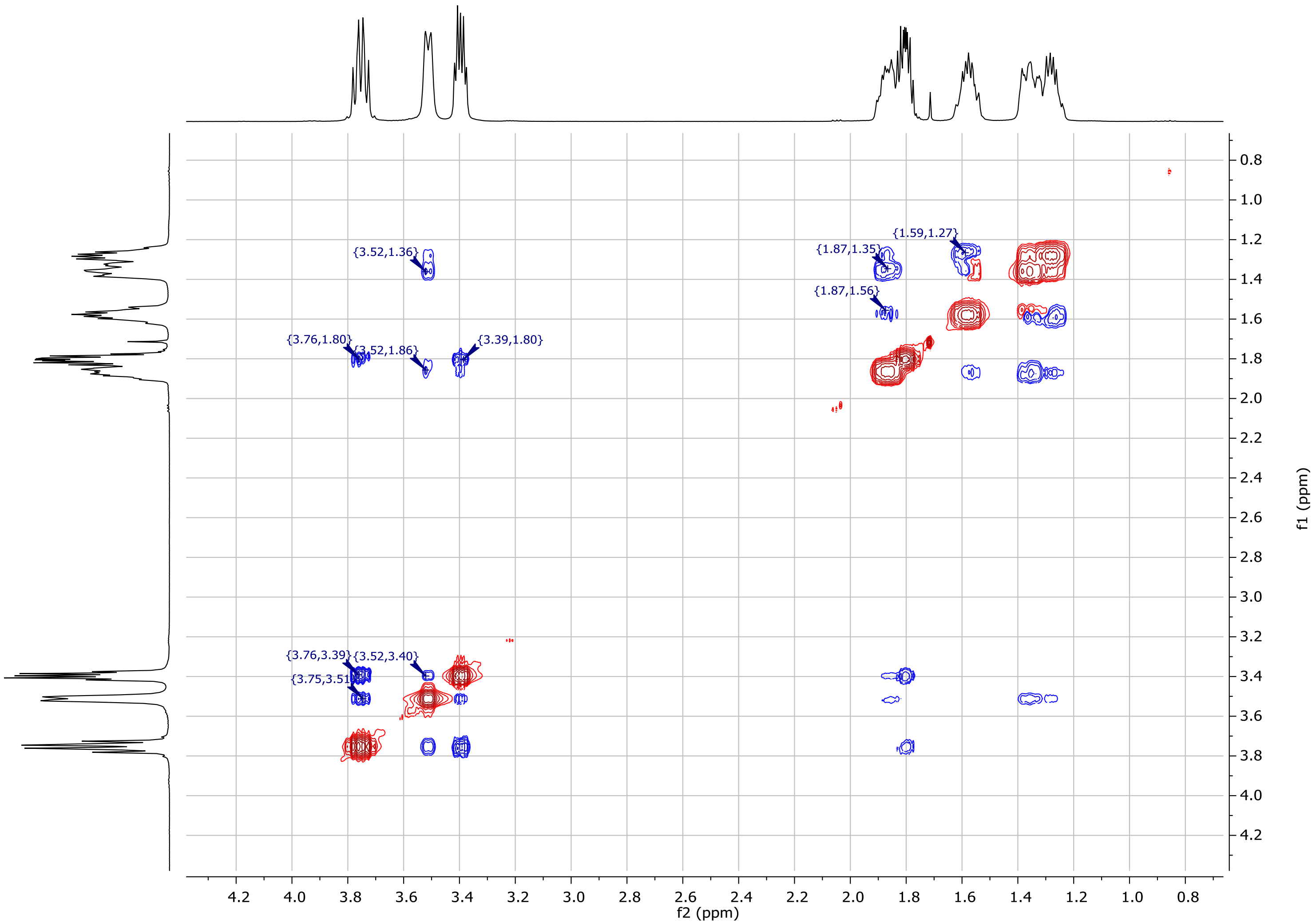

Figure S16 ^{1}H-^{1}H NOESY NMR of *cis*-*anti*-*cis*-DCH14C4 **1b**

6. TGA/DSC analysis of DCH14C4

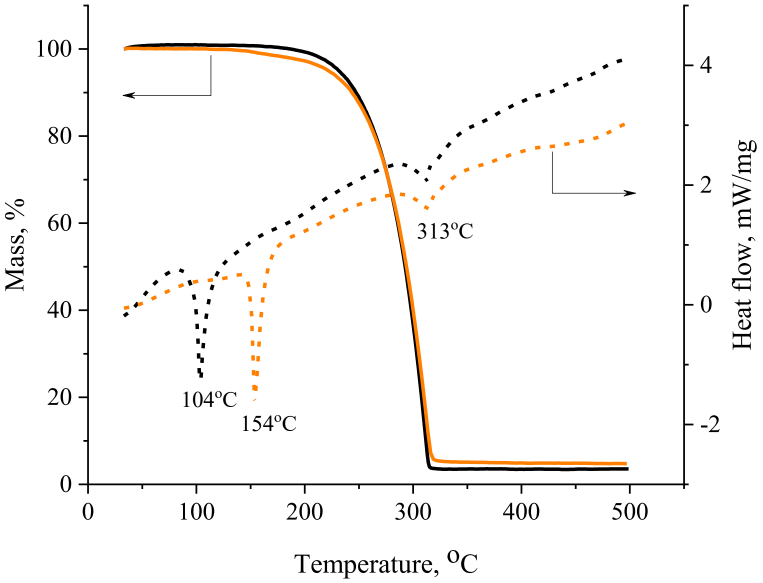

Figure S17 Simultaneous thermal analysis of *cis-syn-cis-* (black curves, **1a**) and of *cis-anti-cis-* (orange curves, **1b**) isomers of DCH14C4. Solid lines relate to TGA and and dash lines – to DSC analysis. The sharp endothermal peaks in the temperature range of 100-150°C correspond to melting points of the isomers

7. FTIR-spectra of DCH14C4

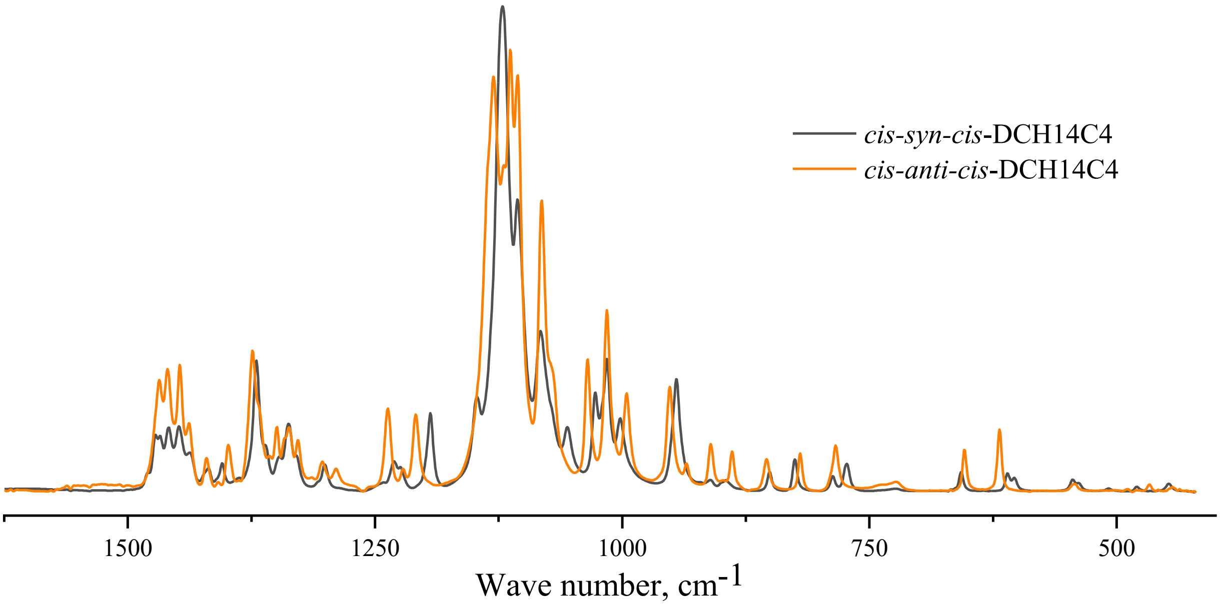

Figure S18 FTIR spectra of *cis-syn-cis*-DCH14C4 **1a** (black line) and *cis-anti-cis*-DCH14C4 **1b** (orange line)

8. References

S1. G. W. Buchanan, K. Bourque, J. W. Bovenkamp, A. Rodrigue and R. A. B. Bannard, *Tetrahedron Lett*., 1984, **25**, 3963; https://doi.org/10.1016/0040-4039(84)80041-6.

S2. O. M. Vilkova and V. V. Yakshin, *J. Anal. Chem.*, 2003, **58**, 27; https://doi.org/10.1023/A:1021877929903.

S3. O. A. Zakurdaeva and S. V. Nesterov, *J. Radioanal. Nucl. Chem.*, 2015, **303**, 1737; https://doi.org/10.1007/s10967-014-3799-1.